PUBLICATIONS OF THE ASTRONOMICAL SOCIETY OF THE PACIFIC
100: 986–992, August 1988

SMALL-SCALE KINEMATIC STRUCTURES IN RING NEBULAE AROUND WOLF-RAYET STARS

YOU-HUA CHU*

Department of Astronomy, University of Illinois, 1011 West Springfield Avenue, Urbana, Illinois 61801

Received 1988 February 29, revised 1988 April 29

ABSTRACT

Four ring nebulae around galactic Wolf-Rayet stars have been observed with echelle spectrographs in the long-slit mode: NGC 2359, NGC 3199, NGC 6888, and RCW 58. The spatial resolution of these observations is seeing limited at ~ 1″–3″, which is almost two orders of magnitude improvement from the previous Fabry-Perot scanner observations. To avoid large geometric corrections, the slit positions were placed as close to the central stars as possible. The results show that the ejecta-type nebula RCW 58 is a clumpy shell expanding regularly at ~ 110 km s^{-1}, as opposed to the chaotic expansion concluded from the earlier Fabry-Perot observations. For the three windblown bubbles, NGC 2359, NGC 3199, and NGC 6888, the small-scale structures revealed in the echelle data can explain the apparently discrepant expansion velocities derived from the previous large-aperture Fabry-Perot observations.

Key words: Wolf-Rayet stars–ring nebulae–H II regions–kinematics

I. Introduction

Wolf-Rayet (W-R) stars are often surrounded by ring-shaped nebulae (e.g., Johnson and Hogg 1965; Smith 1967; Chu 1981; Heckathorn, Bruhweiler, and Gull 1982). The nature of these ring nebulae has been determined by using the internal motions derived from Fabry-Perot scanner observations (Chu, Treffers, and Kwitter 1983, and references therein). According to the major mechanism of formation, the ring nebulae have been classified into three categories: radiatively excited H II regions, stellar ejecta, and windblown bubbles (Chu 1981). Among these three types of rings, the H II regions are quiescent and their dynamic ages are larger than the lifetime of the W-R phase (a few times 10^5 yr), while the other two types are characterized by supersonic expansions with dynamic ages less than the lifetime of the W-R phase. The stellar ejecta appear to have chaotic patterns of internal motion which have been used to distinguish them from the windblown bubbles (Chu 1981).

The Fabry-Perot scanner observations have provided such diagnostic information but sometimes have failed to reveal the velocity pattern accurately and unambiguously. For example, M1-67 and RCW 58, two ejecta-type rings, actually contain *regularly* expanding shells, as shown in slit spectroscopy with high spatial resolution (Solf and Carsenty 1982; Smith *et al.* 1988). These results are contrary to the expectation of chaotic internal motion concluded from the large-aperture Fabry-Perot observations (Chu and Treffers 1981; Chu 1982). Furthermore, the Fabry-Perot observations of RCW 104 (Chu 1982) failed to detect the high-velocity ($\Delta V = -50$ to -120 km s^{-1}) knots near the filamentary edge of this windblown bubble (Goudis, Meaburn, and Whitehead 1988).

Therefore, it is worthwhile to examine the W-R rings with high spatial resolution to supplement the previous low-resolution Fabry-Perot observations and to study the small-scale kinematic structures. In this paper we report the long-slit echelle observations of NGC 6888 in the [O III] line and NGC 2359, NGC 3199, and RCW 58 in the Hα and [N II] lines. The observations are described in Section II, and the small-scale kinematic structures of these four nebulae are presented in Section III. Finally, in Section IV we discuss the differences in the results derived from the high-resolution slit spectroscopy and the large-aperture Fabry-Perot scanner and their implications.

II. Observations

The observation of NGC 6888 was obtained with the echelle spectrograph and a long-focus camera on the 4-m telescope at Kitt Peak National Observatory (KPNO) in September 1987. The instrumental FWHM at the [O III] λ5007 line is 10 ± 0.5 km s^{-1} and the inverse dispersion is ~ 2.5 Å mm^{-1}. A TI CCD was used with 2 × 2 binning; the final 400 × 400 data array had 0.″33 $pixel^{-1}$ perpendicular to the dispersion and ~ 4.6 km s^{-1} $pixel^{-1}$ along the dispersion. The cross-disperser grating was

*Visiting Astronomer, Cerro Tololo Inter-American Observatory and Kitt Peak National Observatory, National Optical Astronomy Observatories, operated by the Association of Universities for Research in Astronomy, Inc., under contract with the National Science Foundation.

replaced by a plane mirror and a postslit interference filter to isolate a single order centered on 5007 Å so that a long slit could be used. In this setup the useful spatial dimension was limited by the size of the CCD chip to be 132″. A slit width of 1″ was used.

The observations of NGC 2359, NGC 3199, and RCW 58 were obtained with the echelle spectrograph and the Air Schmidt camera on the 4-m telescope at Cerro Tololo Inter-American Observatory (CTIO) in January 1988. The instrumental FWHM at the Hα and [N II] lines is 19 ± 1 km s^{-1} and the inverse dispersion is ~ 9.5 Å mm^{-1}. A GEC CCD was used to record the data; the 385 × 576 data array has 0.″635 $pixel^{-1}$ perpendicular to the dispersion and ~ 9.2 km s^{-1} $pixel^{-1}$ along the dispersion. The cross-disperser grating was replaced by a plane mirror and postslit interference filter centered at the Hα line. A 78 Å wide Hα filter was used so that both [N II] λλ6548,6584 lines could be observed at the same time. The CCD chip covers ~ 4′; however, there is a fair amount of vignetting in the outermost 30″. A 1.″6 slit width was used for the CTIO observations.

Thorium-argon lamp exposures were used in the wavelength calibration and line-curvature correction. The telluric OH lines provide an additional check of the wavelength calibration. The telluric Hα line is blended with the nebular Hα component; however, the other observations taken during the same night show that the surface brightness of the telluric Hα is as weak as that of the OH lines at 6553.6 Å and 6577.3 Å, compared to the nebular component. We used the software package IRAF (Interactive Reduction and Analysis Facility) for data reduction and AIPS (Astronomical Image Processing System) for further analysis.

The ring nebulae are brighter at the edge; however, the expansion near the projected edge is almost tangential to the line of sight, and a large geometrical correction is needed to derive the expansion velocity from the observed radial velocities. To avoid such geometric correction, the slit positions in our observation were selected as close to the center of expansion, the central W-R star, as possible. The journal of observations is given in Table I. The echellograms are presented in Figure 1.

III. Small-Scale Kinematic Structures

The distances and sizes of the four W-R ring nebulae are tabulated in Table II. NGC 2359, NGC 3199, and NGC 6888 are windblown bubbles, while RCW 58 contains a conspicuous ring of stellar ejecta inside a windblown bubble (Chu *et al.* 1983). The spatial resolution afforded by the echelle setting is 1″–3″ and is ≪ 0.1 pc for these four nebulae. This is almost 2 orders of magnitude improvement from the previous Fabry-Perot observations made with 1′–2′ apertures. It is possible to examine the small-scale kinematic structures in these echelle data. These four nebulae are described individually below.

A. *NGC 2359*

Our echellogram of NGC 2359 was taken with a 4′-long slit NS oriented and passing through the central WN5 star HD 56925. The velocity structure is by no means a well-defined expansion. There is one stationary component present throughout the slit extent; it is presumably from the ambient unperturbed medium. The shell components have small velocity differences from the stationary component. The largest line split detected is a component which is blueshifted by ~ 28 km s^{-1} at a position 65″ S of the W-R star.

The velocity structure shown in the echellogram can explain the discrepant expansion velocities derived previously using different instruments with different spatial

TABLE I

Journal of Observations

Nebula Name	Offset from WR Star	Slit Width/ Pos. Angle	Exposure Time (s)	Observatory	Date of Obs.
NGC 2359	---	1.″6 / 0°	900	CTIO	1/9/88
NGC 3199	---	1.″6 / 0°	1200	CTIO	1/9/88
NGC 6888	---	1″ / 140°	1200	KPNO	9/2/87
RCW 58	---	1.″6 / 90°	600	CTIO	1/5/88
RCW 58	10″E, 90″S	1.″6 / 0°	1300	CTIO	1/9/88
RCW 58	10″E	1.″6 / 0°	2400	CTIO	1/10/88

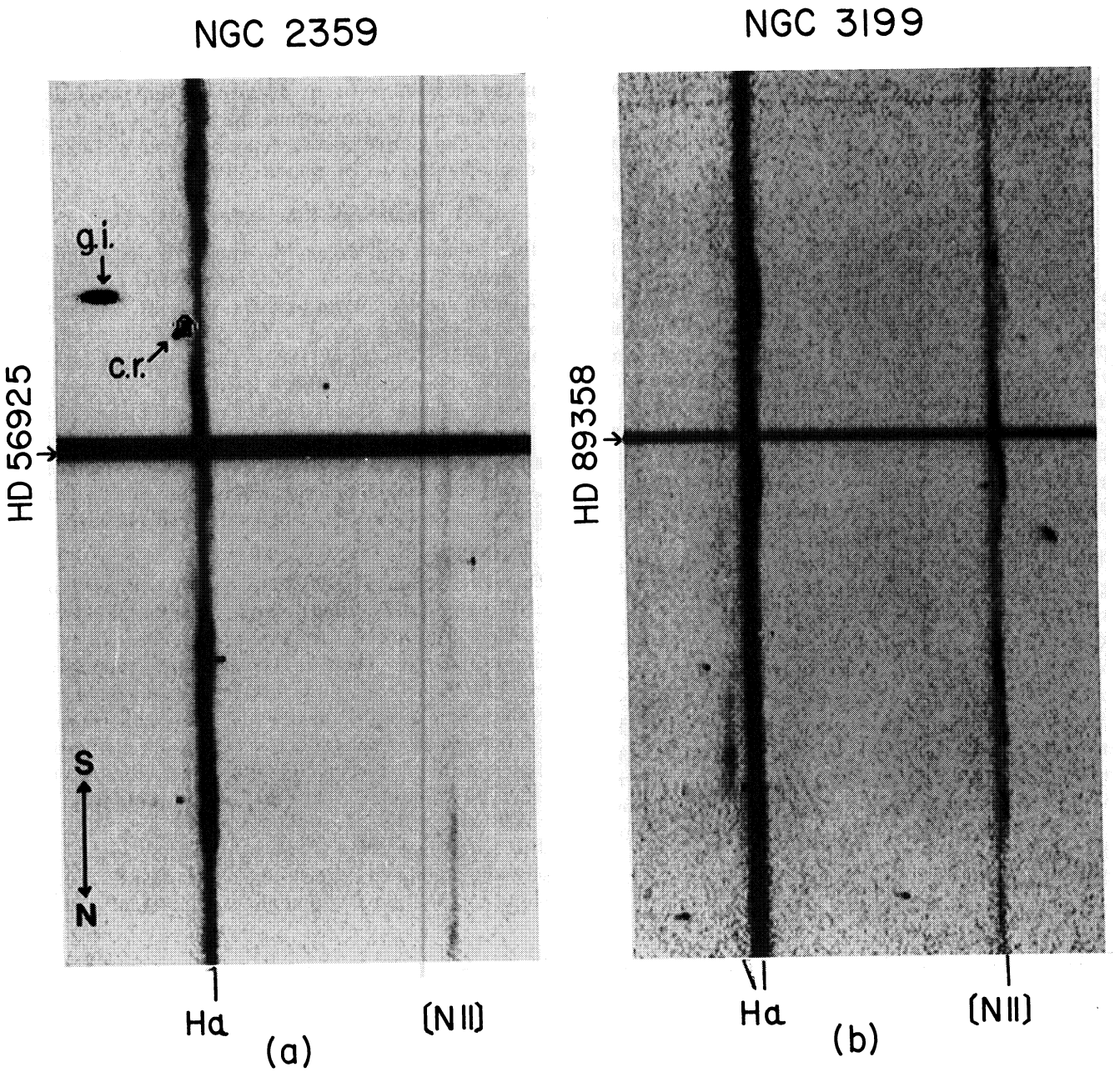

FIG.. 1–(a) Hα and [N II] λ6584 lines of NGC 2359. The wavelength increases toward the right, and south is up. The length of the scale indicator corresponds to 30″ in the Y direction and 432 km s^{-1} in the X direction. The dark horizontal band is the spectrum of the central WM5 star HD 56925. The short horizontal bar at the upper-left corner is the reflected ghost image of the stellar spectrum below. The faint narrow lines are airglow lines; their identification is given in (c). The blob at ~ 30″ S of HD 56925 is caused by a cosmic-ray hit. (b) Hα and [N II] lines of NGC 3199. The scales are the same as in (a). The dark horizontal band is the spectrum of the central WN star HD 89358. The faint blueshifted component is best seen in the Hα line, while the bright stationary and redshifted components are best seen in the [N II] line.

resolution and coverage: 55 ± 25 km s^{-1} (Lozinskaya 1973), ~ 15 km s^{-1} (Pismis, Recillas-Cruz, and Hasse 1977), 15–30 km s^{-1} (Schneps 1979), 18 km s^{-1} (Treffers and Chu 1982), and 30 km s^{-1} (Goudis, Hippelein, and Münch 1983). Although each group argued that their expansion velocity was the most accurate and representative, it is clear that the expansion itself is not regular enough to have a unique expansion velocity. Since expansion velocities are often parameterized to be one-half of the maximum velocity difference in the nebula or the difference between the extreme velocities and the systemic velocity, it is understandable that the expansion velocity of NGC 2359 has been reported to be 15–30 km s^{-1}. To make matters worse, the nebulosity outside the bubble of NGC 2359 does not have a uniform velocity, e.g., see positions 1, 15, and 18 by Goudis *et al.* (1983). It

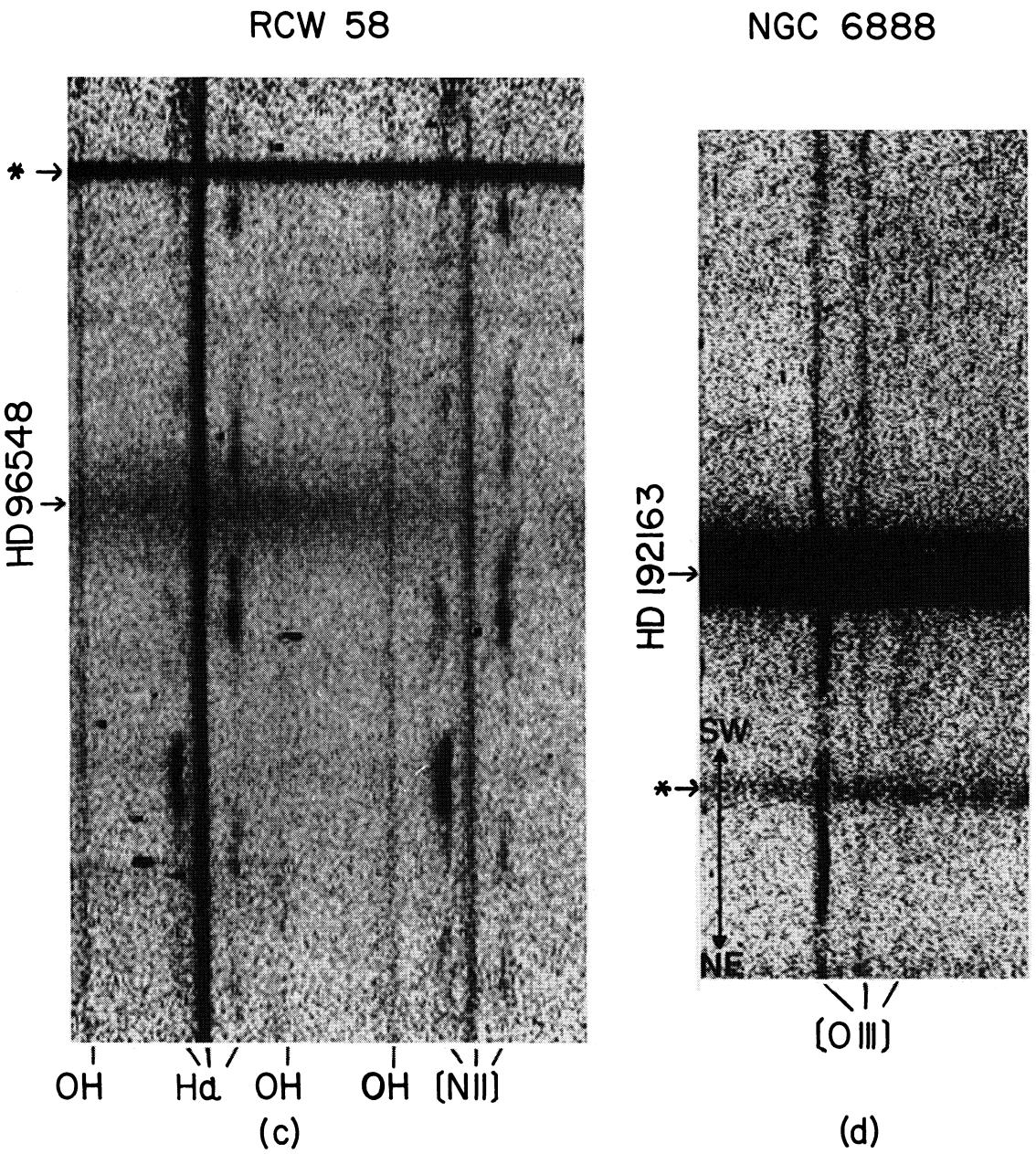

FIG. 1–(c) Hα and [N II] lines of RCW 58. The scales are the same as in (a). The slit position is offset to 10″ E of the central star HD 96548, still stray starlight leaked into the slit and the stellar Hα emission left a broad horizontal band near the center. The stellar spectrum on the top is from a star 77″ S, 11″ E of HD 96548. The OH lines are OH(6-1)P1 λ6553.6, OH(6-1)P2 λ6568.8, and OH(6-1)P1 λ6577.3, respectively. (d) [O III] λ5007 line of NGC 6888. The broad horizontal band is the spectrum of the central star HD 192163, and the narrower band below is a field star. The length of the scale indicator corresponds to 30″ in the Y direction and 418 km s^{-1} in the X direction.

is conceivable that the Fabry-Parot scanner observations are contaminated by an unknown amount of background emission at unknown velocities. Future observations should be planned to cover a large area with arc-sec resolution and should try to map out the velocity fields of both the bubble and the background nebulosity.

B. *NGC 3199*

The expansion of NGC 3199 is quite nonuniform (Chu 1982), and our new echellogram demonstrates this effect particularly well. There is a stationary interstellar component, a bright redshifted component, and a faint blueshifted component. The redshifted component, the back side of the shell, has a variable separation from the stationary component; the maximum separation is ~ 45 km s^{-1} at 35″ S of the WN8 star HD 89358. The blueshifted component is most unambiguously detected at 80″ N of the star with a velocity separation of −82 km s^{-1} from the stationary component. Unfortunately, the slit

TABLE II

Physical Properties of the Observed WR Ring Nebulae

	NGC 2359	NGC 3199	NGC 6888	RCW 58
Distance*	5 kpc	3.3 kpc	1.2 kpc	3 kpc
Angular Size	4!5	16'x20'	12'x18'	7'x9'
Expansion Vel.	15-30 km/s	irregular	75-90 km/s	~110 km/s

* from Chu, Treffers, and Kwitter 1983.

only covers a small segment of NGC 3199, and it is not certain whether this blue component is the approaching side of the shell or an irrelevant background component. Further high-resolution observation mapping both the shell and its vicinity is needed. Clearly, no single expansion velocity can be assigned to NGC 3199 from the expansion structure shown in the echellogram.

C. *NGC 6888*

The echelle spectrum was taken with the slit centered on the WN6 star HD 192163. Three velocity components were detected: the middle one corresponds to the ambient or background interstellar material, the bluest component to the approaching hemisphere, and the reddest component to the receding hemisphere. The velocity structure supports the "simple expanding shell" conclusion derived by the previous investigators (e.g., Lozinskaya 1970; Treffers and Chu 1982). The velocity (V_{LSR}) of the interstellar component is at -1 ± 5 km s^{-1}, consistent with the previous measurement of 2 ± 5 km s^{-1} (Treffers and Chu 1982). The expansion velocity is $\sim$ 75–90 km s^{-1}. There is a 10%–15% expansion velocity variation over the section covered by our slit, and this intrinsic variation can account for the discrepancies among the previous measurements of the expansion velocity.

There are clumps on the approaching side of the shell, and the sizes of the clumps are $\leq 20''$. For observations with large apertures, e.g., 1′ by Johnson and Songsathaporn (1981) and 2′ by Treffers and Chu (1982), complex velocity structures are often seen near the edge of the shell. These complex structures may be produced by dense clumps projected along the line of sight, giving uneven weighting to the velocity profiles.

The velocity widths of the approaching side appear narrower than those of the receding side. The approaching side is bright enough to allow measurements of velocity widths; the turbulent FWHM there is $\sim$ 17 km s^{-1}, about 20% of the expansion velocity. The ratio of the FWHM of the turbulent velocity to the expansion velocity may be a promising way to distinguish between a fast windblown bubble and a slow supernova remnant. This will be discussed in a future paper.

Note: At the completion of this paper, we received a preprint by A. P. Marston and J. Meaburn who had found similar velocity structures for NGC 6888 using long-slit echelle observations in the Hα and [N II] lines.

D. *RCW 58*

In the earlier Fabry-Perot observations (Chu 1982), RCW 58 was reported to have a chaotic velocity pattern. However, the recent high-resolution data of Smith *et al.* (1988) demonstrate that RCW 58 is actually a shell expanding regularly at 87 ± 3 km s^{-1} with a systemic velocity V_{LSR} of -3 ± 2 km s^{-1}.

In our echellograms three components are detected: a constant-velocity component with uniform surface brightness, a clumpy blueshifted component, and a clumpy redshifted component. The clumpy components apparently correspond to the front and back sides of the shell of stellar ejecta, the clumpy ring in the Hα image of RCW 58 (Chu 1982). The stationary component corresponds to the ambient or background interstellar medium. These identifications are supported by the [N II]/Hα ratios; [N II]/Hα is higher in the shell components than in the interstellar component, consistent with the chemical abundance measurements (Kwitter 1984). The largest separation between the blue and red components is about 220 km s^{-1}, corresponding to an expansion velocity of 110 km s^{-1}. It is worth noting that the stationary component is blueshifted by $\sim$ 10 km s^{-1} from the average velocity of the shell. This could mean (1) the clumpy shell of the stellar ejecta is moving through the ambient interstellar material, (2) the interstellar component is along the line of sight but not physically associated with RCW 58, or (3) the ejection is asymmetric. The complex Fabry-Perot line profiles are caused by the uneven weighting of the velocities where dense clumps are present. The expansion of the ejecta is pretty regular.

The velocity of the stationary component is at V_{LSR} of 0 $\pm$ 5 km s^{-1}, in good agreement with the value found by Smith *et al.* (1988). The expansion velocity of 110 km s^{-1} which we measure is from the center of RCW 58 without geometric correction, while Smith *et al.*'s 87 $\pm$ 3 km s^{-1} is extrapolated from the expansion near the southern edge of RCW 58. The difference in these expansion velocities may be due to the nonspherical geometry of RCW 58.

IV. Discussion

As described in Section III, most of the seemingly discrepant internal motions of W-R ring nebulae can be explained by instrumental resolution and characteristics. Below we will compare the observations taken with large-aperture Fabry-Perot scanners and long-slit spectrographs, discuss how the high-resolution results affect the classification scheme of W-R rings (Chu 1981), and suggest an optimal way to study the kinematics.

A. *Fabry-Perot Scanners vs. Long-Slit Spectrographs*

One major difference between the Fabry-Perot scanner observations and the long-slit spectroscopic observations is the spatial resolution. The Fabry-Perot scanner observations usually have 30″–2′ entrance apertures, while the ring nebulae have angular sizes of about 5′–20′. The long-slit spectroscopic observations usually use $\sim$ 1″ slit width, and the spatial resolution is limited by the seeing, a few arc sec at most. A line profile is the convolution of a velocity profile with an emissivity distribution along the line of sight, integrated within the aperture. When the size of the entrance aperture is a significant fraction (e.g., 20%) of the nebula, or when the entrance aperture encompasses many dense cells with large differential velocities, the observed line profiles no longer represent straightforward velocity fields. The Fabry-Perot scanner and the long-slit spectroscopic observations of M1-67 and RCW 58 provide the most dramatic demonstration of the effect of spatial resolution.

Spatial information is essential when the expansion is irregular or when the background nebulosity has variable velocities. It is important to follow each velocity component spatially. If the velocity components from adjacent apertures do not vary continuously, it is a good indication that the spatial resolution is too low to derive unambiguous information. By the same token, if the line profiles sampled from an expanding shell do not behave as expected, it would be wise to observe with higher spatial resolution.

Another drawback of the Fabry-Perot scanners is their limited free spectral range, which is usually $\sim$ 150 km s^{-1} for the observations of the W-R ring nebulae. Under such a condition, a high-velocity feature may be assigned a lower velocity with the opposite sign, and a weak component may be mistaken as a noise bump and ignored. This free spectral range problem does not become apparent until the high-velocity knots are detected in RCW 104 (Goudis *et al.* 1988). These knots have projected radial velocities of -55 to -125 km s^{-1} relative to the systemic velocity of $V_{LSR} \sim 45$ km s^{-1}. In the Fabry-Perot profiles taken at similar positions (Chu 1982), there is indeed a hint of a component at a V_{LSR} of -100 km s^{-1} (3W1N in Fig. 5); however, the highest velocity knots would have blended into the main component from the adjacent spectral order.

B. *Classifying W-R Ring Nebulae*

One important thing we have learned from the high-resolution observations of W-R ring nebulae is that the internal motions of the stellar ejecta are more organized than what has been interpreted from the previous Fabry-Perot data. It is fortuitous that the ejecta-type ring nebulae have been correctly identified in the Fabry-Perot data. This is because the combination of rapid expansion and clumpy structure is a unique property of stellar ejecta. The rapid expansion is a result of the ejection velocity which is of the order of the escape velocity on the stellar surface, and the clumpy structure is a result of the strong Rayleigh-Taylor instability (Jones, Smith, and Straka 1981). The H II region-type W-R rings do not have rapid expansion; if there are any clumps at all, they are interstellar material and their velocities are low (usually subsonic). The windblown bubbles do not suffer Rayleigh-Taylor instability unless the stellar-wind luminosity increases with time or the ambient density drops off rapidly, e.g., on the surface of a molecular cloud (Weaver *et al.* 1977).

The classification criteria for the ejecta-type W-R rings have to be modified. The previous "chaotic" velocity field criterion for the ejecta-type W-R rings is an observational artifact of the clumpy structure in the shell due to Rayleigh-Taylor instability. Therefore, the main criterion differentiating windblown bubbles and stellar ejecta shells should be in the density structure within the shell. The ejecta-type nebulae are clumpy at a scale size of ≤ 0.1 pc and the condensations follow a regular expansion pattern, while a windblown bubble may reflect the ambient interstellar environment and expand irregularly, and the denser material should move at a smaller velocity.

Note that sometimes there is no clear distinction between bubbles and ejecta. The stellar ejecta are short-lived, and they evaporate on time scales of a few times 10^3 yr, or a few times 10^4 yr if they are embedded within windblown bubbles (Chu 1981). Therefore, the older stellar ejecta have to coexist with windblown bubbles; for example, RCW 58 has a shell of ejecta with a dynamic age of 2–3 $\times$ 10^4 yr inside a windblown bubble. For any shells older than a few times 10^4 yr, there is no obvious kinematic or morphological distinction between a pure windblown bubble and a bubble contaminated with stellar ejecta. Therefore, the "windblown bubble"-type W-R

rings do not exclude the possibility of containing stellar ejecta; they are not intended to exclude ejecta anyway.

Most of the W-R ring nebulae are unaffected by the modification of the classification criteria; an exception is NGC 6888. The velocity structure of NGC 6888 is somewhat similar to that of RCW 58. It is possible that NGC 6888 contains a significant amount of stellar ejectum, as well as interstellar material, in which case NGC 6888 may better be classified as a bubble/ejecta type. This is another case in which ejectum cannot be unambiguously distinguished from bubble.

C. *Optimal Observations of Nebular Kinematics*

The galactic W-R ring nebulae have angular sizes ~ 5′–20′. Observers used to shy away from the high-resolution slit spectrographs for fear that undersampling and low surface brightness might cause problems. However, the sensitive modern detectors make it possible to observe them with long but narrow slits, and the results have revolutionized our understanding of stellar ejecta and revealed the small-scale structures in windblown bubbles.

Clearly we have benefited from the high spatial resolution. Any future observations should try to maximize the spatial coverage while maintaining a high spatial resolution. Increasingly available imaging Fabry-Perot interferometers are an excellent way to map the velocity structures. However, pilot long-slit spectroscopic observations should be sampled beforehand to determine the velocity range so that an adequate free spectral range and optimal velocity scanning step size can be selected.

I wish to thank Drs. G. H. Jacoby and R. C. Kennicutt for agreeing to use spare telescope time on these W-R rings and Dr. J. R. Dickel for reading and commenting on the manuscript. This research is supported in part by NSF grant AST 86-12021.

REFERENCES

Chu, Y.-H. 1981, *Ap. J.*, **249**, 195.
———. 1982, *Ap. J.*, **254**, 578.
Chu, Y.-H., and Treffers, R. R. 1981, *Ap. J.*, **249**, 586.
Chu, Y.-H., Treffers, R. R., and Kwitter, K. B. 1983, *Ap. J. Suppl.*, **53**, 937.
Goudis, C. D., Hippelein, H., and Münch, G. 1983, *Astr. Ap.*, **117**, 127.
Goudis, C. D., Meaburn, J., and Whitehead, M. J. 1988, *Astr. Ap.*, **191**, 341.
Heckathorn, J. N., Bruhweiler, F. C., and Gull, T. G. 1982, *Ap. J.*, **252**, 230.
Johnson, H. M., and Hogg, D. E. 1965, *Ap. J.*, **142**, 1033.
Johnson, P. G., and Songsathaporn, R. 1981, *M.N.R.A.S.*, **195**, 51.
Jones, E. M., Smith, B. W., and Straka, W. C. 1981, *Ap. J.*, **249**, 185.
Kwitter, K. B. 1984, *Ap. J.*, **287**, 840.
Lozinskaya, T. A. 1970, *Sov. Astr.-A.J.*, **14**, 98.
———. 1973, *Sov. Astr.-A.J.*, **17**, 317.
Pismis, P., Recillas-Cruz, E., and Hasse, I. 1977, *Rev. Mexicana Astr. Ap.*, **2**, 209.
Schneps, M. H. 1979, Ph.D. dissertation, Massachusetts Institute of Technology.
Smith, L. F. 1967, Ph.D. dissertation, Australian National University.
Smith, L. J., Pattini, M., Dyson, J. E., and Hartquist, T. W. 1988, *M.N.R.A.S.*, in press.
Solf, J., and Carsenty, U. 1982, *Astr. Ap.*, **116**, 54.
Treffers, R. R., and Chu, Y.-H. 1982, *Ap. J.*, **254**, 569.
Weaver, R., McCray, R., Castor, J., Shapiro, R., and Moore, R. 1977, *Ap. J.*, **218**, 377.